



RESEARCH ON RECONSTRUCTION ALGORITHM OF COMPLETE TOOTH MODEL

Engineering

Wenjing Shi

School of computer science and software engineering, Tianjin Polytechnic University, Tianjin, 300387, China

ABSTRACT

In a computerized dental prosthetic system, a complete digital 3D dental model relates to subsequent dental implants, implants, orthodontics, and biomechanical analysis. Therefore, this paper proposes a set of system flow and algorithm for each stage to generate a high-accuracy, complete-data tooth model. This article is mainly from the CT and optical scanning of these two different data acquisition tooth model for follow-up operations, including: reconstruction of CT data, the separation of the gums and crowns of the optical scanning tooth model, data registration, co-segmentation, model integration and so on. The 3D digital tooth model required for the computational aided design is finally generated. Theory and experiment show that the process and algorithm of this paper can achieve a good reconstruction of the dental model, and it is fast and easy to operate.

KEYWORDS

Stomatology, 3D digitization, model reconstruction, different types of data

Introduction

Three-dimensional imaging techniques commonly used in the oral field include laser scanning (physical dental laser scanning or intraoral laser scanning) and computed tomography (CT) [1]. At present, the complete three-dimensional model of teeth is mainly obtained through segmentation and reconstruction of oral CT images [2, 3]. Although the dental model obtained from dental CT image reconstruction contains complete three-dimensional information, due to the low precision of CBCT scan and the influence of the slice thickness and metal artifacts, the surface accuracy of the crown is insufficient. The goal of dental implants and orthodontic treatment is to reconstruct the tooth and balance the occlusal contact. However, inaccurate crown dimensions will result in incorrect orthodontic diagnosis. At the same time, in order to establish a three-dimensional model of the teeth under different periodontal patterns during the treatment process, it is necessary to repeatedly perform an oral CT scan on the patient, which will cause radiation damage to the patient.

The use of laser scanning images to establish a three-dimensional crown model has some limitations in clinical applications. The laser scan image mainly contains the three-dimensional information of the crown of the patient, which has an image resolution of ten micrometers, and the reconstructed model has high precision, but tooth root information of the tooth cannot be obtained. Therefore, if the collision detection in the digital orthodontics process mainly refers to the information of the crown, it is difficult to determine the potential collision of the root due to the movement of a large distance. And if there is a lack of information on the relative position between the root and maxilla or mandible during treatment, this can lead to large root movements, bone resorption, or windowing of the cortical bone [4]. Thus, it is very necessary to develop a dental 3D model reconstruction system based on oral CT and laser scanning.

2. Related work

Zhou Jing et al. (2010), Gao Yi et al. (2011), Tang Min et al. (2012) and Guo Hongming et al. (2013) separately reported the use of custom reference planes (Constructed from the three gingival margin lines with the lowest gingival height in the dentition) for segmentation and tailoring of post-registration optical scans and CBCT dentition models. The optical crown data and CBCT root data are retained, and the data retained by the two are combined to complete crown and root data fusion. This method simplifies the software operation process, which is convenient for clinicians to operate. However, the separation of crowns and cormorants is not complete, and there is a difference between the fusion data and the actual tooth anatomy, and the morphology of the crown and root junctions is lost. In 2013, Barone et al. [11] used the level set algorithm to extract tooth outlines from CBCT images and reconstruct a 3D model. It was then fused with the optically scanned three-dimensional coronal data to generate an all-tooth model. However, the author did not describe the specific method of data integration. In 2012 Kihara et al. [12] used commercial software for manual fusion of roots and crowns. In 2014, Yau et al. [13] applied the Delaunay-based region growing algorithm to achieve

crown and root data fusion. These methods have made progress in the fusion of different sources of crown and root data. However, the level of automation is low and involves a lot of manual operations, which increases the complexity of the overall tooth structure. These shortcomings are the bottleneck of the current development of orthodontics. In 2015, Jung et al. [14] proposed a new flow and method for tooth model generation. First, a single tooth was segmented from a CT image and then registered with optical data. And CT tooth is used to guide the optical scanning tooth model for the separation of crown and gum. Finally, the CT model and the single crown model were registered and fused to realize the regeneration of the dental model. In 2017, Zhao et al. [15] proposed a registration method for continuous curvature algorithm. The three-dimensional model after the registration is used to extract the exact crown and boundary lines, offset and projection of the boundary lines, generation of crown and root boundary lines, and model clipping. The curvature continuity algorithm is used to realize the natural transitional suturing of crown and root models from different sources to achieve crown and root construction.

As can be seen from the above, obtaining a complete, high-precision dental model composed of CT and optical scan data has the following problems: 1) It is very difficult to obtain a single tooth model directly from a CT slice. 2) The registration of the tooth model after CT slice reconstruction and the optical scanning obtained tooth model is inaccurate. 3) The accuracy and resolution of CT data and optical scan data are quite different. And how to achieve the natural transition of the two models is the technical difficulty of crown and root data fusion. Therefore, in view of these difficulties, this paper proposes a dental model reconstruction system based on oral CT and laser scanning.

3. System flow and analysis

The main purpose of this paper is to generate a 3D digital tooth model with high precision and complete data. So the overall system flow is shown in figure 1.

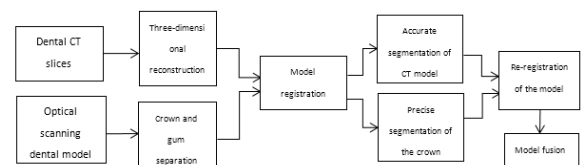


Fig. 1 The overall flow chart of the system

3.1 Reconstruction of the CT model

The three-dimensional reconstruction methods of medical images mainly include three-dimensional volume rendering and three-dimensional surface rendering. The Marching Cubes algorithm (MC algorithm) proposed by W. Lorensen [16] et al. in 1987 is the most typical surface rendering method. Its principle is to calculate geometric primitives from three-dimensional data, usually triangular facets or surfaces to calculate the vertical graphical coordinate points

and corresponding normal vectors. Then using computer three-dimensional rendering technology, according to the three-dimensional coordinates and the normal vector, draw a realistic three-dimensional image. the steps for finding isosurfaces can be described as follows:

- Three-dimensional discrete rules data field layered reading;
- Scan two layers of data and construct voxels one by one. The eight vertices in each voxel are taken from two adjacent layers.
- Compare each corner function value of a voxel with a given isosurface value to obtain the configuration index value of the voxel;
- Look up the index of the voxel with the intersection point of the isosurface according to the configuration index value;
- Calculate the intersection of voxel edge and isosurface by linear interpolation method;
- Find the normal vector at each corner of the voxel and the normal vector at each vertex of the triangle patch.
- Draw the isosurface.

Cube has rotational symmetry, rotation does not affect the isosurface topology. In addition, all Insides become Outside, while all Outsides change to Inside, and the connection of the isosurfaces does not change (Inversion symmetry). Considering Rotation symmetry and Inversion symmetry, we can use 15 basic cubes to cover all possible 256 cases. As shown in figure 2.

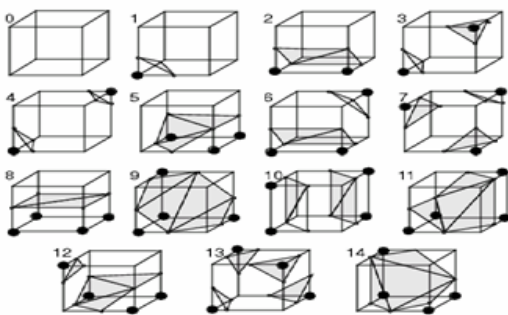


Fig. 2 15 basic Cubes situations

Based on these 15 basic Cubes, we can create a Look-up Table. The length of the table is 256, which records the isosurface connection in all cases. The index value is used to query a look-up table with a length of 256, and the edge numbers of the three vertices of the isosurface triangle are obtained. After the edge number is obtained, linear interpolation is performed on the edge to obtain the coordinates of the vertex of the triangle.

$$P = P_1 + \frac{(\text{isovalue} + V_1)(P_2 - P_1)}{(V_2 - V_1)} \quad (1)$$

Where P is the coordinates of the isocenter, P1 and P2 are the coordinates of the two endpoints, V1 and V2 are the gray values of the two endpoints, isovalue represents the threshold;

The gray-gradient-based normal vector estimation method is a very effective iso-surface normal vector calculation method. First, the grayscale gradient $g = (g_x, g_y, g_z)$ at the vertex (i,j,k) of the voxel is calculated using the grayscale difference.

$$g_x = \frac{s(i+1, j, k) - s(i-1, j, k)}{2}$$

$$g_y = \frac{s(i, j+1, k) - s(i, j-1, k)}{2} \quad (2)$$

$$g_z = \frac{s(i, j, k+1) - s(i, j, k-1)}{2}$$

The normalization of g results in $(\frac{g_x}{|g|}, \frac{g_y}{|g|}, \frac{g_z}{|g|})$ as the unit normal vector on (i,j,k). Then, the normal vectors of the eight vertexes on the voxels are linearly interpolated to obtain the normal vectors at the vertices of the triangles on the edges of the voxels.

$$N = N_1 + \frac{(\text{isovalue} + V_1)(N_2 - N_1)}{(V_2 - V_1)} \quad (3)$$

N is the iso-point normal vector, N1, N2 represent the normal vectors of the two endpoints, V1, V2 represent the gray values of the two endpoints, and isovalue represents the threshold. The results of reconstruction of CT tooth slices in this paper are shown in figure 3.



Fig. 3 Three-dimensional model reconstructed from CT slices

3.2 The separation of teeth and gums from an optical scan model

A fast segmentation algorithm with high segmentation precision is proposed in this paper in combination with the grid extraction algorithm[17] and interactive marker control algorithm [18].The algorithm idea is described as follows:

- (1) Grid extraction. Mesh extraction of optically scanned tooth models to appropriately reduce the number of meshes;
- (2) Mesh smoothing. The Laplacian smoothing algorithm is used to smooth the triangular mesh to eliminate the noise of the mesh.

The STL file obtained by laser scanning often has noise. In order to eliminate the noise and improve the accuracy of the segmentation, the Laplacian smoothing algorithm is used in the smooth processing of triangular teeth meshes. The algorithm first finds a set of 1 neighborhood vertices for each vertex V_i of the mesh $G = \langle V, E \rangle$, and its 1 neighborhood is defined as the union of the points that are all edges with the point V_i :

$$L^1(V_i) = \{V_j | \exists \text{edge}(V_i, V_j)\} \quad (4)$$

Then we construct an array of 1 neighborhoods Array[n] for each vertex V_i , where n is the number of 1 neighborhood vertices for each vertex V_i . The coordinates of V_i are modified according to the average value of all vertex coordinates in the 1 neighborhood array Array[n] (ie, using an umbrella operator $U(V_i)$) And according to the actual operation to carry out a number of iterations.

$$U(V_i) = \frac{1}{n} \sum_{k=0}^{n-1} Adj_k(V_i) \quad (5)$$

Curvature calculation. As a face set segmentation algorithm, the curvature of the surface is estimated to be between two adjacent patches. In this algorithm, the boundary of the dental digital model is determined by the degree of bending of two adjacent patches. The curvature calculation method is as follows:

We set two triangular patches $f1, f2$ whose unit normal vectors are $n1$ and $n2$, respectively, and let $f1$ and $f2$ share the same AC. AB is a non-common edge of one of the triangular patches. The function of the relative degree of bending of the two patches $f1$ and $f2$ marked can be defined as [18]:

$$H(f_1, f_2) = H(f_2, f_1) = \begin{cases} \frac{n_1 * n_2 - 1}{2} & n_1 * AB \leq 0 \\ \frac{1 - n_1 * n_2}{2} & n_1 * AB > 0 \end{cases} \quad (6)$$

- (3) Stack operation
Stack iteration process: Determine whether the stack is empty. If it is not empty, the top element of the stack is popped. Find the neighboring and visited=FALSE patch of the patch and push it onto the stack.
- (4) Regional growth. All patches of the tooth grid are accessed and mesh patches are grouped according to the minima rule [19] to achieve tooth separation.

The results of the tooth model segmentation are shown in figure 4.

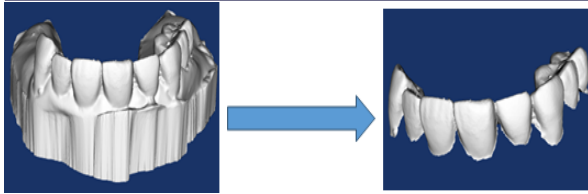


Fig. 4 Separate crown and gum from optical scan data

3.3 Image Registration

The registration of this paper is divided into two procedures: initial and precise registration. Since the registration will not be accurate if the angle between the initial point cloud and the target point cloud exceeds 15 degrees, this paper uses manual selection of feature points for initial registration. Manually selecting several points with features on the CT (reconstructed) model, then selecting corresponding feature points on the optical scan crown in turn, and then registering the results. We set a uniform scale factor before registration to solve the problem of the different resolutions of the two data. The method of manually selecting the feature points has a small amount of calculation and can basically achieve the registration of the two kinds of data, but the accuracy of registration has a greater connection with the skill level of the operator. In order to solve the influence of such human factors, during the registration phase, feature points are automatically selected. The random sampling method is used to obtain $p(p \ll n)$ sampling points to reduce the amount of data calculation, and use the K-D tree to accelerate the search for the corresponding point pairs, and introduce the scale transformation parameters to iterate the seven degrees of freedom, which can not only improve the accuracy of registration but also improve the time efficiency of registration, and ultimately achieve the two Merging images.

$$f(\lambda, R, T) = \sum_{i=1}^n ||Q_i - (\lambda R X_i + T)||^2 = \min \quad (7)$$

Where λ is the scale parameter, and X_i is the point set of p .

3.4 Common Segmentation of Models

The main goal of this step is to separate the parts of a single crown from two different data sets at the same time. From section 3.2 we can see that we have separated the crown from the gums, but the bottom edge of the crown is still affected by the gums. Therefore, in order to make the segmentation of the crown more accurate, we use the CT-reconstructed tooth model to guide the accuracy segmentation of the optical crown. In Section 3.3, we have achieved accurate registration of the CT reconstruction model and the optical crown. In this section, we use the similarity and dissimilarity of the two to accurately segment the crown. Keeping the same part of the optical crown and the CT dental model, and removing the areas where the two are not the same, a small amount of gingival part on the edge of the optical crown can be separated.

After separating the excess gums, we can obtain a more accurate crown model, and then separate a single crown model and guide the exact cutting of the CT model. After separating the individual crowns, we re-registered them so that the CT slices were aligned with the individual crowns. Then the CT crowns were used to cut the optical crowns so that the contours were mapped on each CT slice. The results are shown in figure 5.

These contours are set to a uniform gray value, and then a Marching cubes algorithm is used for three-dimensional reconstruction, so that a high-precision tooth model is separated from the CT slice. However, this is only reconstructing the crown portion of the tooth. For the root portion of the CT, we use the classical Level set method to segment and select the last contour as the initial contour, which avoids manual selection of the initial contour.

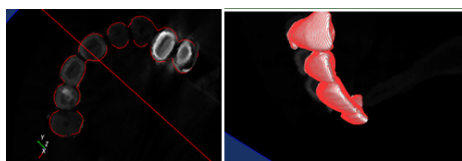


Fig.5 The mapping of optically scanned crowns on CT slices

The Level Set Method (LSM) was originally proposed by Osher et al. [20] and was mainly used to solve the flame evolution process following the thermodynamic equation. The core idea of the level set method is to use a zero-level set of $n + 1$ dimensional functions to represent n -dimensional functions. The final evolution results are obtained by obtaining the positions of the points of the high-dimensional function on the zero-level surface. For a closed two-dimensional curve, the zero-level surface of the three-dimensional surface can be used for implicit expression. Therefore, the two-dimensional curve motion is converted into a three-dimensional surface motion. The change of the curve at each moment can be expressed by the zero-level set of the surface.

The mathematical form of the evolution of the level set can be explained and deduced from the partial differential angle. Given the level set function is $\phi(C, t)$ then the zero level set of the curve $C(t)$ at time t can be expressed as $\phi(C(t), t) = 0$ Differentiating the above formula, we can get:

$$\frac{\partial \phi}{\partial t} + \nabla \phi \cdot \frac{\partial C}{\partial t} = 0 \quad (8)$$

Where $\nabla \phi$ is the gradient of the level set function ϕ If we set the arc length parameter of curve C to s , we can see from the definition of the level set function that the tangential component $\frac{\partial \phi}{\partial s}$ of ϕ with respect to C is zero, so we can get the following formula:

$$\frac{\partial \phi}{\partial s} = \frac{\partial \phi}{\partial x} \cdot \frac{\partial x}{\partial s} + \frac{\partial \phi}{\partial y} \cdot \frac{\partial y}{\partial s} = \langle \nabla \phi, \frac{\partial C}{\partial s} \rangle \quad (9)$$

$$\text{which is: } \langle \nabla \phi, \frac{\partial C}{\partial s} \rangle = 0 \quad (10)$$

Equation (3) shows that the gradient of the level set function is perpendicular to the tangent of the curve, which is the same as the normal direction of the curve. In general, the unit normal vector N that defines the level set curve is:

$$N = -\nabla \phi / |\nabla \phi| \quad (11)$$

Combining equations (1), (2), (4), the level set evolution equation is as follows:

$$\frac{\partial \phi}{\partial t} = -\nabla \phi \cdot \frac{\partial C}{\partial t} = -\nabla \phi \cdot F \cdot N = F |\nabla \phi| \quad (12)$$

Where F is the speed function of the level set.

3.5 The fusion of models

In this paper, Delaunay-based region growing (DBRG) algorithm is used to fuse the re-aligned laser scanning crown and oral CT image reconstruction tooth, so as to establish a complete three-dimensional dental model [1,21]. Apexes of the crown model of the reconstructed laser scanning image after registration are searched for the closest point of 1 to 15 points in the CT image reconstruction tooth model. The vertices obtained by removing these points from the tooth model are the tooth root apexes of the CT image reconstruction, and the root models can be reconstructed using these vertices. The result of the fusion is shown in figure 6.

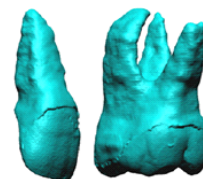


Fig. 6 merging result

4. Conclusion

This paper have proposed a method flow based on dental CT and optical scanning tooth model 3D reconstruction. The experimental results have verified that this method can effectively use the crown of the optical crown and the CT slice to reconstruct the three-dimensional

model of the intact tooth. The reconstruction of the dental model using this method has a higher accuracy of the crown, contains the information of the root, and the operation is simple and can be used for the auxiliary design of the invisible braces without brackets.

5. References

- [1]. Dongxia, Z., Yangzhou, G., Jing, X. Three-dimensional tooth model reconstruction based on fusion of dental computed tomography images and laser-scanned images. *Journal of Biomedical Engineering*, 34(1):2-14 (2017).
- [2]. Yangzhou, G., Zeyang, X., Jing, X. Toward accurate tooth segmentation from computed tomography images using a hybrid level set model. *Med Phys*, 42(1): 14-27 (2015).
- [3]. Zeyang, X., Yangzhou, G., Jing, X. Crown segmentation from computed tomography images with metal artifacts. *IEEE Signal Process Lett*, 23(5): 678-682 (2016).
- [4]. Ning, D., Dawei, L., Xu, Y. Research and primary evaluation of an automatic fusion method for multisource tooth crown data. *National Natural Science Foundation of China*, (2016).
- [5]. Enciso, R., Memon, A., Mah, J. Three-dimensional visualization of the craniofacial patient: volume segmentation, data integration and animation. *Orthod Craniofac Res*, 6(Suppl 1):66-71,179-182 (2003).
- [6]. Macchi, A., Carrafello, G., Cacciafesta, V. Three-dimensional digital modeling and setup. *Am J Orthod Dentofacial Orthop*, 129(5):605-610 (2006).
- [7]. jing, Z., Hongming, G. 3D visualization and setup of digital model integrating roots and jaws. *Beijing Journal of Stomatology*, 18(1): 14-17 (2010).
- [8]. yi, G., Hongming, G., Jiemin, Z. Application of 3D integrating model containing jaws and roots in invisalign design. *Beijing Journal of Stomatology*, 19(5):276-179 (2011).
- [9]. Min, T., Hongmin, G., Yuxing, B. Application of integrated digital maxillofacial model in computer aided design of individualized lingual brackets. *Chinese Journal of Stomatology*, 47(8):501-504 (2012).
- [10]. Hongming, G., Xiaojia, Z., Yong, Z. Exposure of the root in virtual treatment on laser-scanned dental model. *Beijing Journal of Stomatology*, 21(3):156-158 (2013).
- [11]. Barone, S., Paoli, A., Razionale, A. V. Creation of 3D multi-body orthodontic models by using independent imaging sensors. *Proceedings of the 9th ACM SIGGRAPH conference on virtual-reality continuum and its applications in industry. Sensors*, 13(2):2033-2050 (2013).
- [12]. Kihara, T., Tanimoto, K., Michida, M. Construction of orthodontic setup models on a computer. *American Journal of Orthodontics and Dentofacial Orthopedics*. 141(6):806-813 (2012).
- [13]. Yau HT, Yang TJ, Chen YC. Tooth model reconstruction based upon data fusion for orthodontic treatment simulation. *Computers in Biology and Medicine*. 48:8-16 (2014).
- [14]. Wonhyung Jung, Seyoun Park, Hayong Shin. Combining volumetric dental CT and optical scan data for teeth modeling. *Computer-Aided Design*. 24-37 (2015).
- [15]. Z Yijao, L yi, S Yuchun. Three-dimensional data fusion method for tooth crown and root based on curvature continuity algorithm. *journal of PEKING University(Health sciences)*, 49(4): 719-723 (2017).
- [16]. Lorensen, W.E., Cline, H.E. Marching Cubes: A High Resolution 3D Surface Construction Algorithm [A]. *SIGGRAPH'87 Proceedings*, 163-169 (1987).
- [17]. Schroeder, W. J., Zarge, J. A., Lorensen, W. E. Decimation of triangle meshes. *Acem Siggraph Computer Graphics*, 26(2):65-70 (1992).
- [18]. Li Chengjun, Zhang Chi, Wang guoping. Fast Marker- Controlled Interactive Mesh Segmentation. *Acta Scientiarum Naturalum Universitatis Pekinesis*. 42(5):662-667 (2006).
- [19]. Donald D Hoffman, Manish Singh. Saliency of visual parts. *Cognition*, 63(1):29-78 (1997).
- [20]. CHENH, JAINAK. Tooth contour extraction for matching dental radiographs. *Proceedings of the 2004 17th International Conference on Pattern Recognition*. Washington, DC: IEEE Computer Society, 3: 522-525 (2004).
- [21]. Kuo C C, Yau H T. A delaunay-based region-growing approach to surface Reconstruction from unorganized points. *Comput Aided Des*, 37(8): 825-835 (2005).